Predictions of a Turbulent Separated Flow Using Commercial CFD Codes

Gianluca Iaccarino
Center for Turbulence Research,
Stanford University,
Stanford, CA 94305-3030

Numerical simulations of the turbulent flow in an asymmetric two-dimensional diffuser are carried out using three commercial CFD codes: CFX, Fluent, and Star-CD. A low-Reynolds number k-ϵ model with damping functions and the four-equation $\overline{v'^2}-f$ model are used; the first one is available as a standard feature in all the codes, the $\overline{v'^2}-f$ model was implemented using the User Defined Routines. The flow features a large recirculating zone due to the adverse pressure gradient in the diffuser; the $\overline{v'^2}-f$ predictions agree very well with the experiments both for the mean velocity and the turbulent kinetic energy. The length of the separation bubble is also computed within 6 percent of the measured value. The k-ϵ calculations do not show any recirculation and the agreement with the measurements is very poor. The three codes employed show very similar characteristics in terms of convergence and accuracy; in particular, the results obtained using the $\overline{v'^2}-f$ are consistent in all the codes, while appreciable differences are obtained when the k-ϵ is employed. [DOI: 10.1115/1.1400749]

1 Introduction

Computational Fluid Dynamics tools are becoming standard in many fields of engineering involving flow of gases and liquids; numerical simulations are used both in the design phase to select between different concepts and in the production phase to analyze performance. Industrial CFD applications require high flexibility in the grid–generation procedure for complex configurations, short turn around time, and easy–to–use environments. At present, several commercial packages are available for the CFD industrial community; these packages are usually integrated systems which include a mesh generator, a flow solver, and a visualization tool. Often the numerical techniques adopted in these CFD codes are well accepted algorithms published in the open literature; the selection of one technique with respect to others is usually based on robustness and reliability.

There have been few attempts in the literature to compare the performance of these codes; laminar and turbulent test cases have been proposed to several CFD code vendors by the Coordinating Group for Computational Fluid Dynamics, of the Fluids Engineering Division of ASME[1]. A series of five benchmark problems were calculated, with all the mesh generation and simulations performed by the vendors themselves; only two of the problems required turbulent simulations. The first problem is the flow around a square cylinder; the flow is unsteady and all the codes predicted reasonably well the measured Strouhal number. However, poor accuracy resulted in the prediction of the details of the wake flow field. It was also noted that, depending on the code used (and assuming grid-converged results) the *same* k-ϵ model predicted very different results. The reasons for this difference can be different grids, no demonstration of grid convergence, different implementations of the models, and different boundary conditions. It must also be pointed out that the prediction for this problem is strongly affected by the treatment of the stagnation point region. As shown by Durbin [2], the k-ϵ models predict a *spurious* high level of turbulent kinetic energy in this region.

The other turbulent problem reported by Freitas [1] was the three-dimensional developing flow in a 180 degrees bend. In this case all the solutions reported were unsuccessful in predicting the measured data in the bend region and the resolved structure of the flow field was significantly affected by the choice of the turbulence model.

The uncertainties associated with (i) different computational grids, (ii) boundary conditions definition, (iii) convergence, and (iv) numerical schemes do not allow drawing specific conclusions about the codes used, other than the usual conclusion that *further research into more advanced turbulence models for use in commercial CFD codes is required* [1].

In order to carry out a fair comparison between different CFD codes and to establish definitive conclusions on the state–of–the–art of commercial CFD codes, all the differences $(i$-$iv)$ must be fully addressed and, if possible, eliminated. In the present work, an effort has been made to control all these parameters. The codes available for comparison are CFX, Fluent, and Star-CD. The objective is to compare their predictive capabilities for the simulation of a turbulent separated flow. Several turbulence closures (and near-wall treatments) are available in these codes ranging from k-ϵ-type models to full Reynolds stress models. The main focus of the work is on two models: the k-ϵ low-Reynolds model by Launder and Sharma [3] and the $\overline{v'^2}-f$ by Durbin [4]. In addition, results obtained using different closures are reported.

The k-ϵ model is well described in the literature and has been widely used. Its implementation poses some challenges and it requires the solution of two transport equations with numerically stiff source terms. This model is available in all the codes considered and, although it is not expected to be extremely accurate [5], it provides common ground for comparisons between different codes.

The $\overline{v'^2}-f$ model (implemented in a NASA research code) has been already successfully used for simulating separated flows [4], three dimensional configurations [6] and flows with heat transfer [7]. It is rather complex involving the solution of four differential equations (three transport equations plus an Helmotz-type equations).

The test case analyzed in this study is a two-dimensional turbulent flow in a diffuser. Due to the adverse pressure gradient the flow is separated and a large recirculation bubble is generated. This problem has been selected because a very reliable experimental database is available. Moreover, a detailed Large Eddy

Contributed by the Fluids Engineering Division for publication in the JOURNAL OF FLUIDS ENGINEERING. Manuscript received by the Fluids Engineering Division October 16, 2000; revised manuscript received May 21, 2001. Associate Editor: I. Celik.

Simulation study was carried out at the Center for Turbulence Research and the resulting numerical database is also available for comparison [8].

The objective of the paper is to present a detailed and careful comparison of the simulations performed using three commercial CFD codes. Although the flow under investigation is geometrically simple, it is challenging for turbulence modeling and must be considered as a necessary step to evaluate the merits of different approaches. In addition, its simplicity allows to control all the numerical parameters involved in the simulations and to understand the causes of discrepancy between the codes.

The three CFD codes used are briefly introduced in the next section; the turbulence models with the governing equations are presented in Sec. 3, while results and comparison are in Sec. 4.

2 Numerical Method

The steady Navier-Stokes (NS) equations for an incompressible fluid are considered:

$$\frac{\partial u_i}{\partial x_i}=0 \tag{1}$$

$$u_i\frac{\partial u_j}{\partial x_i}=\frac{\partial}{\partial x_j}\left[(\nu+\nu_t)\frac{\partial u_j}{\partial x_j}\right]-\frac{\partial p}{\partial x_j} \tag{2}$$

where u_i are the mean velocity components, p is the pressure, and ν and ν_t the laminar and turbulent viscosity, respectively. Additional equations for turbulent quantities are considered to compute the eddy viscosity, and are explained in the following section.

All the codes solve the discretized equations in a segregated manner, with the SIMPLE (Semi-Implicit Method for Pressure-Linked Equations) algorithm, or its ''consistent'' variant, SIMPLEC [9], used to achieve the pressure-velocity coupling for stability. In the SIMPLE algorithm, the continuity equation (1) is converted into a discrete Poisson equation for pressure. The differential equations are linearized and solved implicitly in sequence: starting with the pressure equation (predictor stage), followed by the momentum equations and the pressure correction equation (corrector stage). The equations for the scalars (turbulent quantities) are solved after the updating of both pressure and velocity components. Within this loop, the linearized equations for each variable, as they arise, are treated using a linear system solver (i.e., multigrid, Preconditioned Conjugate Gradient, PCG, etc.).

A brief description of the codes is given in the next subsections with emphasis given only to the features required for this study. All the codes allow the implementation of customized models through User Defined Subroutines.

2.1 CFX v4.3. CFX v4.3 is a CFD computer code developed and marketed by AEA Technologies. The code solves the three-dimensional NS equations on structured multiblock grids for both compressible and incompressible flows. Various turbulence models are available ranging from two-equation to complete Differential Reynolds Stress Models (DRSM). CFX uses a SIMPLEC pressure-correction scheme (SIMPLE is also available), and several spatial discretizations which include first-order Upwind Differencing (UD) and QUICK [10]; central differencing is used for the pressure. The linear system arising at each iteration is then solved using a Preconditioned Conjugate Gradient technique.

2.2 Fluent v5.3. Fluent v5.3 is a CFD computer code developed and marketed by Fluent Inc. The code provides mesh flexibility by unstructured meshes. Turbulence closures range from one-equation turbulence model up to DRSM [11].

Fluent employs the SIMPLEC technique and an algebraic multigrid linear system solver to update the solution at each iteration. The QUICK spatial discretization technique is available among others. In particular, a second-order Total Variation Diminishing (TVD) limited discretization for the pressure in the Poisson equation is used [12].

2.3 Star-CD v3.1. Star-CD v3.1 is a CFD computer code developed and marketed by Computational Dynamics Ltd. The code solves the three-dimensional NS equations on unstructured meshes; various linear and non-linear two-equation turbulence models are available [13].

Star-CD uses the SIMPLE technique for velocity-pressure correction and a PCG method to solve the implicit system of equations; several first and high order spatial discretization schemes can be used including QUICK.

3 Turbulence Modeling

Several turbulence models are available in the codes presented in the previous section. Most of them are derived from the standard k-ϵ model [14] with different treatments of the wall region.

The low-Reynolds model of Launder and Sharma [3] and the $\overline{v'^2}-f$ model [4] are the focus of this work, and are described in detail. Additional simulations are performed with the k-ϵ Two-Layer Model [15], the cubic Non-Linear Eddy-Viscosity (NLEV) k-ϵ Model [16], and the Differential Reynolds Stress Model [13].

The Launder and Sharma k-ϵ model is available as a standard option in all the codes (a slightly different damping function is employed in Star-CD). The $\overline{v'^2}-f$ model has been implemented using the User Defined Subroutines in each of the codes.

3.1 Low-Reynolds k-ϵ Model. The k-ϵ model was introduced by Launder and Spalding [14]. The high Reynolds number version is obtained by neglecting all the terms containing the kinematic viscosity. In the proximity of solid walls, viscous effects become important and this assumption no longer holds. Several modifications have been proposed: in the two-layer formulation [15], a simpler model is used close to the wall (usually a one-equation model) and then the eddy viscosity is patched at a certain distance from the wall; both Fluent and Star-CD offer this option. In the damping functions approach [17] algebraic functions are introduced to correct the behavior of turbulent quantities close to the wall. Several different choices are available in the open literature. All the codes have built-in damping function models; in particular, Fluent has six different versions available. In this work, the model introduced by Launder and Sharma [3], which is available in all the codes, was used.

The k-ϵ equations are:

$$u_i\frac{\partial k}{\partial x_i}=P-\epsilon+\frac{\partial}{\partial x_j}\left[\left(\nu+\frac{\nu_t}{\sigma_k}\right)\frac{\partial k}{\partial x_j}\right]-D \tag{3}$$

$$u_i\frac{\partial \epsilon}{\partial x_i}=\frac{f_1C_{\epsilon_1}P-f_2C_{\epsilon_2}\epsilon}{T}+\frac{\partial}{\partial x_j}\left[\left(\nu+\frac{\nu_t}{\sigma_\epsilon}\right)\frac{\partial \epsilon}{\partial x_j}\right]+E \tag{4}$$

The eddy viscosity is obtained from

$$\nu_t=C_\mu f_\mu kT \tag{5}$$

The damping functions f_1, f_2, and f_μ, the timescale T and the extra source terms D and E are:

$$f_1=1 \tag{6}$$

$$f_2=1-0.3e^{-Re_T^2} \tag{7}$$

$$f_\mu=e^{-3.4/(1+0.02\mathrm{Re}_T)2} \tag{8}$$

$$T=k/\epsilon \tag{9}$$

$$D=2\nu\left(\frac{\partial\sqrt{k}}{\partial x_n}\right)^2 \tag{10}$$

$$E=2\nu\nu_t\left(\frac{\partial^2 u_i}{\partial x_j x_k}\right)^2 \tag{11}$$

where $\mathrm{Re}_T=k^2/\nu\epsilon$ is the turbulent Reynolds number and x_n is the direction normal to walls.

The damping function f_μ used in StarCD is slightly different from that reported by Launder and Sharma [3]. In order to eliminate this possible cause of discrepancy between the codes, the eddy viscosity in StarCD has been computed using a User-Defined Subroutine according to Eq. (5) with f_μ defined as in (8).

The same constants have been used in all the codes, corresponding to the values reported by Launder and Sharma [3]. The implementation of this model is not straightforward because of the presence of the extra-source terms (10) and (11). In particular, the definition of the direction x_n, the normal to the wall, maybe difficult in general geometries and the evaluation of the second derivatives of the velocity vector (Eq. (10)) is computationally expensive. The presence of the molecular viscosity in the expressions (10) and (11) makes the contributions negligible away from the walls. However, their implementation affects the behavior of turbulent quantities in the viscous-dominated near-wall regions.

3.2 $\overline{v'^2}-f$ Model. The $\overline{v'^2}-f$ turbulence model is an alternative to the k-ϵ model and was introduced to model the near-wall turbulence without the use of exponential damping or wall functions. The model requires the solution of four differential equations: the basic equations for k and ϵ are the same as before (Eqs. (3)-(4)) but with the following definitions:

$$f_1 = 1 + 0.045\sqrt{k/\overline{v'^2}} \tag{12}$$

$$f_2 = 1 \tag{13}$$

$$f_\mu = \overline{v'^2}/k \tag{14}$$

$$T = \max\left[\frac{k}{\epsilon}, 6\sqrt{\frac{\nu}{\epsilon}}\right] \tag{15}$$

$$D = 0 \tag{16}$$

$$E = 0 \tag{17}$$

The additional equations model the turbulence velocity scale $\overline{v'^2}$, and its production, kf:

$$u_i\frac{\partial \overline{v'^2}}{\partial x_i} = kf - 6\overline{v'^2}\frac{\epsilon}{k} + \frac{\partial}{\partial x_j}\left[\left(\nu + \frac{\nu_t}{\sigma_k}\right)\frac{\partial \overline{v'^2}}{\partial x_j}\right] \tag{18}$$

$$f - L^2\frac{\partial^2 f}{\partial x_j \partial x_j} = C_1\frac{(2/3 - \overline{v'^2}/k)}{T} + C_2\frac{P}{k} + \frac{5\overline{v'^2}/k}{T} \tag{19}$$

where L is the length scale, defined as

$$L^2 = C_L^2 \max\left[\frac{k^3}{\epsilon^2}, C_\eta^2\sqrt{\frac{\nu^3}{\epsilon}}\right] \tag{20}$$

The eddy-viscosity damping is provided in this case by the presence of $\overline{v'^2}$ (Eq. (14)) instead of k in Eq. (5). In other words, the amount of damping is controlled by the ratio between $\overline{v'^2}$ and k (instead of the turbulent Reynolds number, Re_t, like in the k-ϵ model) which is a measure of the turbulence anisotropy [4]. The other important feature of the $\overline{v'^2}-f$ model is the nonlocality arising from the solution of an elliptic equation for f.

The $\overline{v'^2}-f$ model has been implemented by the author in the three CFD codes described above. Four additional scalars are solved and the diffusion, source, and convective terms are specified according to Eqs. (3)-(4) and (18)-(19). The eddy viscosity is then computed according to Eq. (5) and used in the mean flow Eqs. (1)-(2).

4 Results

Steady flow in asymmetric, two-dimensional diffuser is considered. This problem was a test-case for the 8th ERCOFTAC/IAHR/COST Workshop on Refined Turbulence modeling in Espoo, Finland, 17-18 June 1999.

The geometry is presented in Fig. 1: the inlet conditions are specified as a fully-developed channel flow at Re=20,000 based on the centerline velocity and the channel height. Separate channel flow simulations were carried out using each code and each turbulence model and the resulting profiles are used as inlet conditions for the simulation of the diffuser.

An experimental database is available from Obi et al. [18] and Buice and Eaton [19]. The data include mean and fluctuating velocities at various stations in the diffuser and skin friction data on both walls. The data can be obtained directly from the Web (www.aero.hut.fi/Ercoftac/ws8/case8_2).

A structured grid consisting of 124×65 points in the streamwise and wall normal direction, respectively, has been used. Strong clustering of the grid points at the walls has been used so that the y^+ of the first grid point away from the wall is everywhere less than 1. A detail of the computational grid in the region close to the connection between the channel and the diffuser is included in Fig. 2.

In Table I a summary of the numerical parameters used for the computations is reported.

In Fig. 3, convergence histories for the all simulations are presented. The residuals have been normalized using their values at the first iteration. The convergence levels reached after 3000 iterations are comparable in all the cases. In particular, slightly lower residuals are obtained using the $\overline{v'^2}-f$ in both Fluent and CFX but not in Star-CD. An extensive analysis of the sensitivity of the convergence history to the numerical parameters (listed in Table 1) was outside the scope of the present work and was not

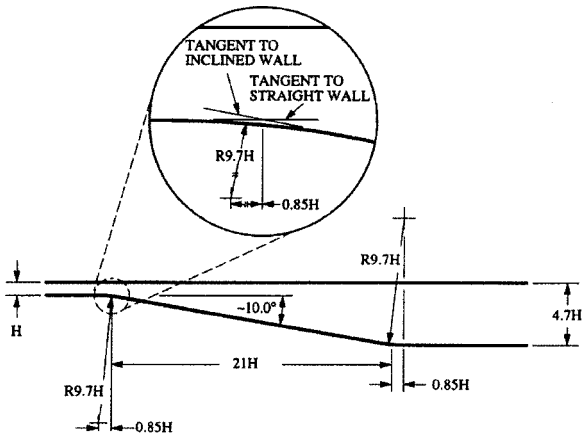

Fig. 1 Asymmetric diffuser geometry

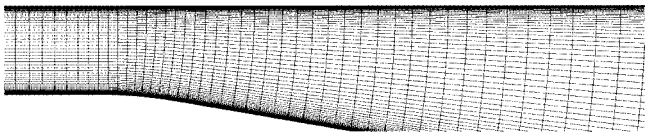

Fig. 2 Computational grid—detail of the channel-diffuser connection

Table 1 Numerical parameters used for the simulations. Legend: U,V: Mean Velocity Components; P: Pressure; TQ: Turbulent Quantities; CD: Central Differencing; UD: Upwind Differencing; TVD: Total Variation Diminishing.

	Spatial Discretization			Pressure Correction	Under-Relaxation		
	U,V	P	TQ		U,V	P	TQ
CFX	QUICK	CD	UD	SIMPLEC	0.65	1	0.6
Fluent	QUICK	TVD	UD	SIMPLEC	0.65	1	0.6
Star-CD	QUICK	CD	UD	SIMPLE	0.70	0.2	0.6

performed. However, the SIMPLEC algorithm used in CFX and Fluent seems to be superior to the standard SIMPLE (also available in the same codes). This technique is not available in Star-CD and the other options available did not give better convergence behaviors. In terms of performance, the unstructured mesh codes (Fluent and StarCD) behaved similarly, with the structured grid code (CFX) being 40 percent faster. The CPU cost of the $\overline{v'^2}-f$ model is about 30 percent more than the k-ϵ model and this is consistent with the fact that two additional differential equations are solved. As it is clear from the Fig. 3, no major differences in terms of convergence speed are observed between the simulations performed using the two turbulence models even if the $\overline{v'^2}-f$ has been implemented as an external customized module.

In Fig. 4 the streamwise velocity contours are reported for the

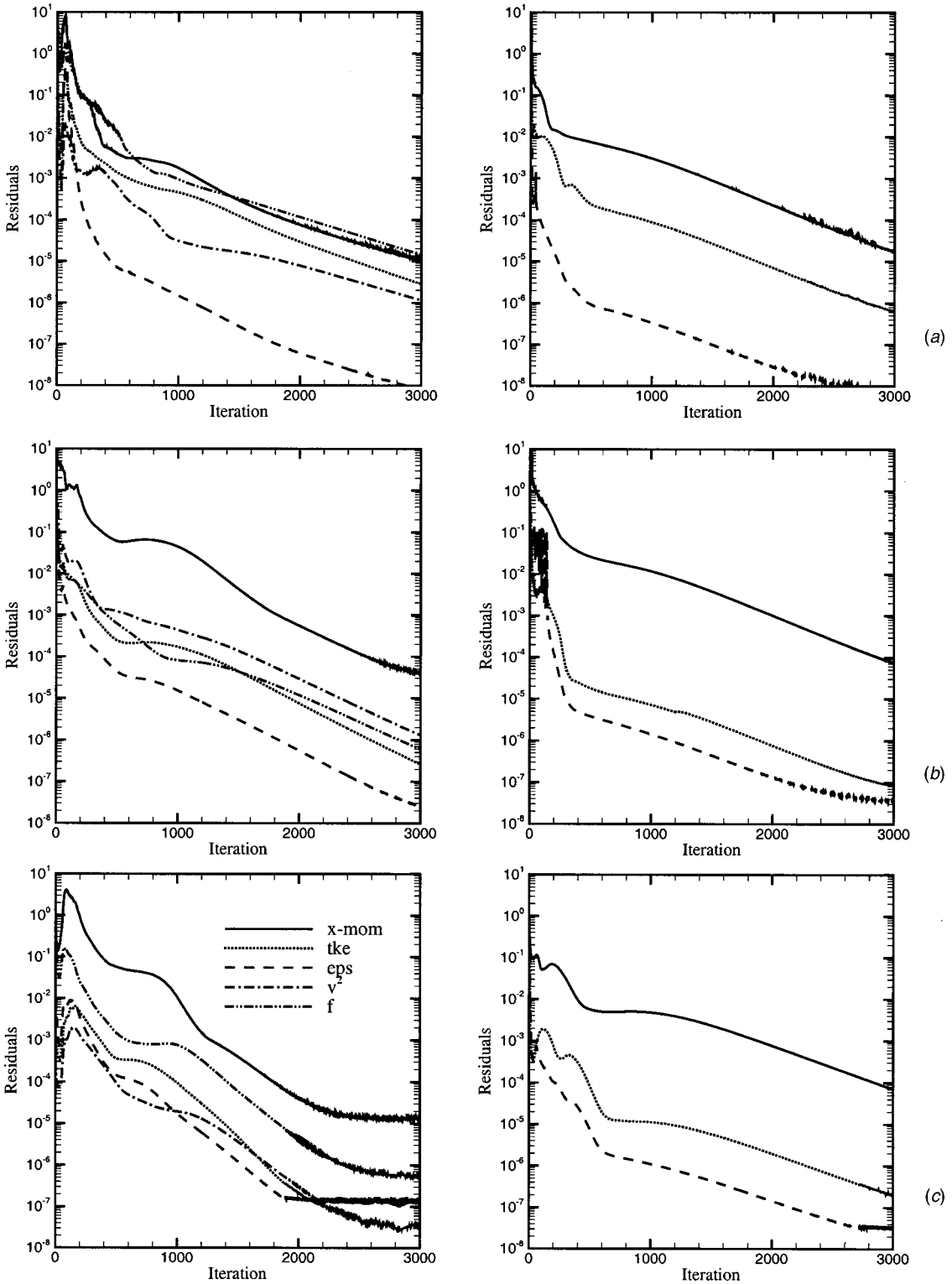

Fig. 3 Convergence history (L_∞ norm). Left column: $\overline{v'^2}-f$ model; right column: low-Reynolds k-ϵ model. (a) CFX v4.3; (b) fluent v5.3; (c) star-CD v3.1.

two models. The results using the $\overline{v'^2}-f$ model show a separation bubble (dashed lines) in qualitative agreement with the experimental findings. This recirculation is not captured by the low-Reynolds k-ϵ model.

The comparison between the computations and the experimental data is reported in Fig. 5 for the streamwise velocity at several stations in the diffuser. The $\overline{v'^2}-f$ results are consistently in good agreement with the measurements for the mean velocity. In par-

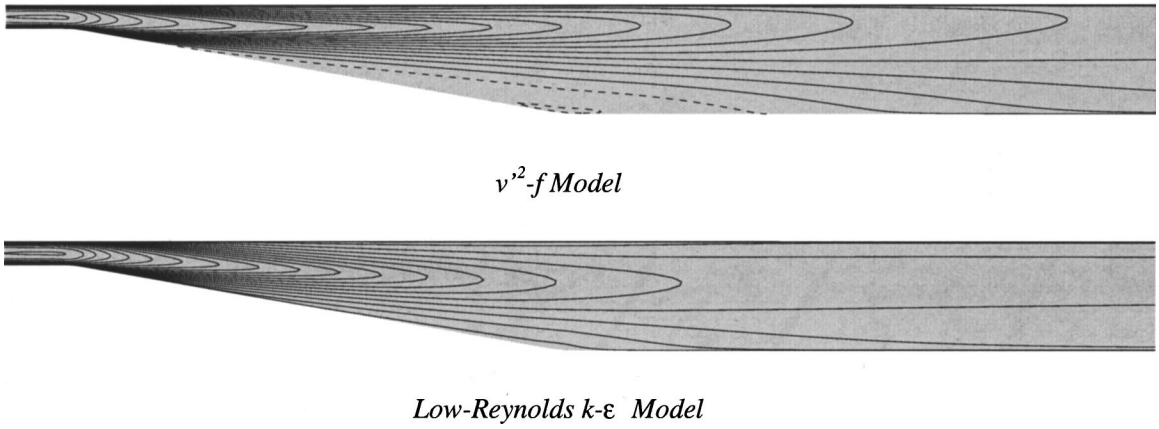

v'²-f Model

Low-Reynolds k-ε Model

Fig. 4 Mean streamwise velocity—CFX. Contour levels Min=−0.05; max=1.0, Δ=0.05 (dashed lines negative values).

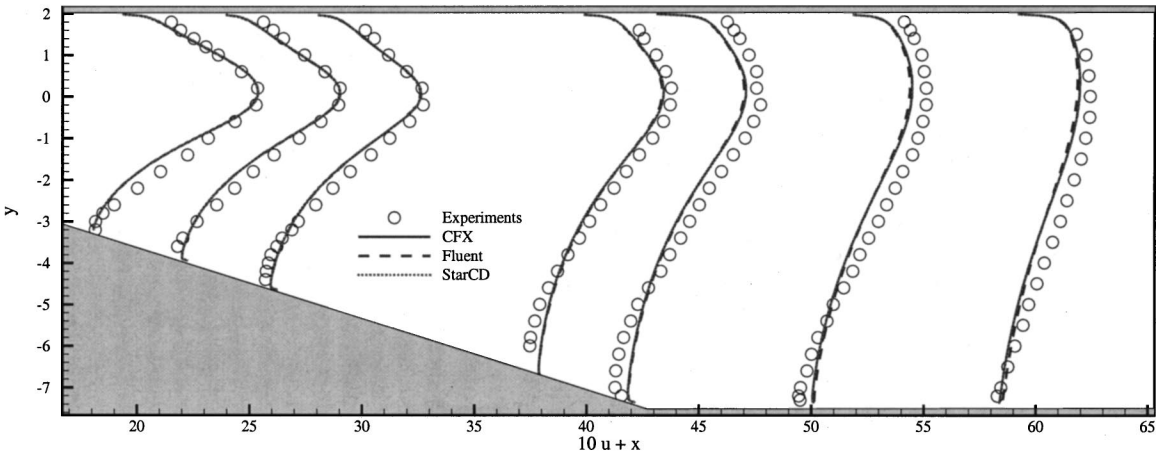

$\overline{v'^2} - f$ *Model*

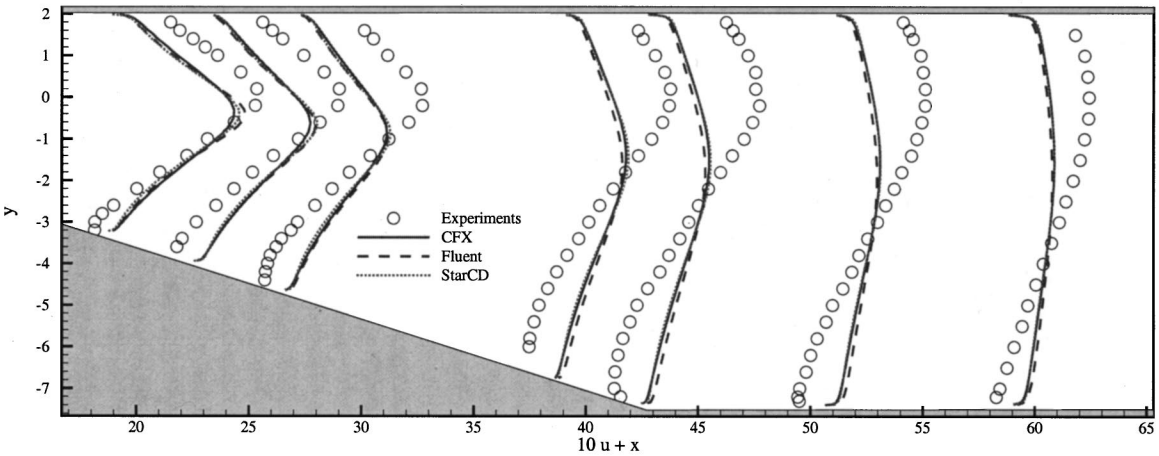

Low-Reynolds k-ε Model

Fig. 5 Streamwise velocity profiles

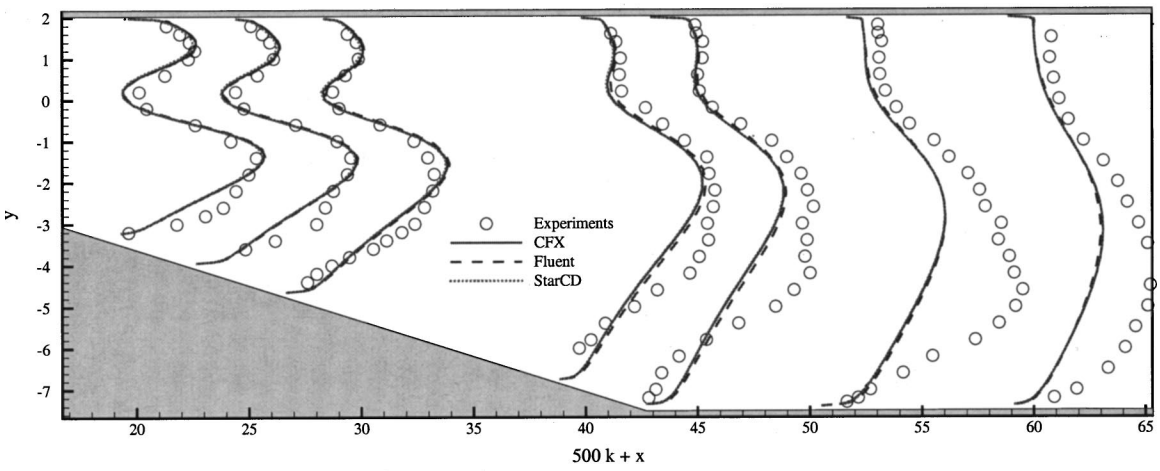

$\overline{v'^2} - f$ *Model*

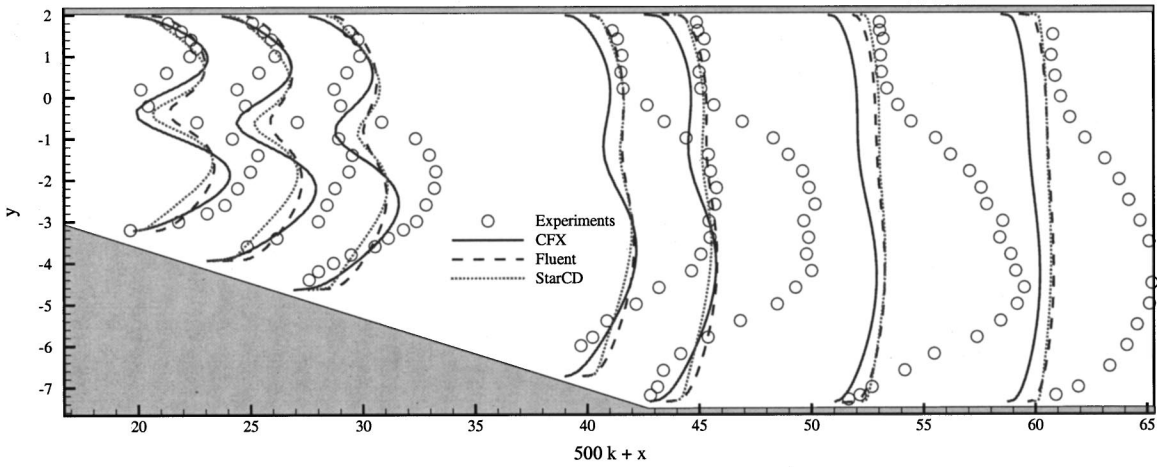

Low-Reynolds k-ϵ Model

Fig. 6 Turbulent kinetic energy profiles

ticular, the separation zone is captured (even if the maximum intensity of the recirculating velocity is underestimated). The predictions using the k-ϵ model are in poor agreement with the data because the model fails to respond correctly to the adverse pressure gradient and misses the separation completely. The comparisons reported in Fig. 6 for the turbulent kinetic energy confirm the quality of the $\overline{v'^2}-f$ predictions as compared to the k-ϵ. The peak of the turbulent intensity is very well predicted by the $\overline{v'^2}-f$ model in the diffuser. However, in the recovery region (after the reattachement) the model underestimates the level of kinetic energy. This is consistent with the $\overline{v'^2}-f$ calculations shown by Durbin [4], the LES results reported by Kaltenbach et al. [8] and with the recent computations presented by Apsley and Leschziner [5] using quadratic and cubic nonlinear k-ϵ models. Possible reasons for this disagreement are the presence of strong three-dimensional effects after the flow reattachement and strong non-equilibrium effects which cannot be correctly accounted for in single–point closures. The results using the k-ϵ model completely fail to capture the asymmetric development of the turbulent kinetic energy and underestimate its magnitude in the diffuser.

The three codes show some differences when the same k-ϵ model is invoked. The disparities are in the mean velocity and especially in turbulent kinetic energy. The very good agreement obtained by using the $\overline{v'^2}-f$ suggests that the differences are not related to the numerical techniques used to discretize the equations but to the implementation of the models. For example, different approximations of the terms in (10)-(11) could lead to the mentioned differences.

In particular, it is worth noting that StarCD and Fluent results are closer to each other (especially for the turbulent kinetic energy) than they are with CFX. This may be related to the fact that both are unstructured mesh codes (whereas CFD is a structured grid solver) and they deal similarly with the issues (mentioned at the end of Sec. 3.1) related to the computation of the cross derivatives in the term D (Eq. (10)) and the evaluation of the wall normal direction. It is also useful to add that the use of the standard f_μ damping function available in StarCD (instead of the one reported in (8)) leads to somewhat different results which no longer agree with the Fluent results.

Finally in Fig. 7 the skin friction coefficients on the lower and upper walls are reported. The separation bubble on the curved wall is indicated by a negative skin friction from $x/H \approx 7$ to $x/H \approx 30$; the $\overline{v'^2}-f$ model predicts the bubble in very close agreement with the experiments. The k-ϵ model fails to predict

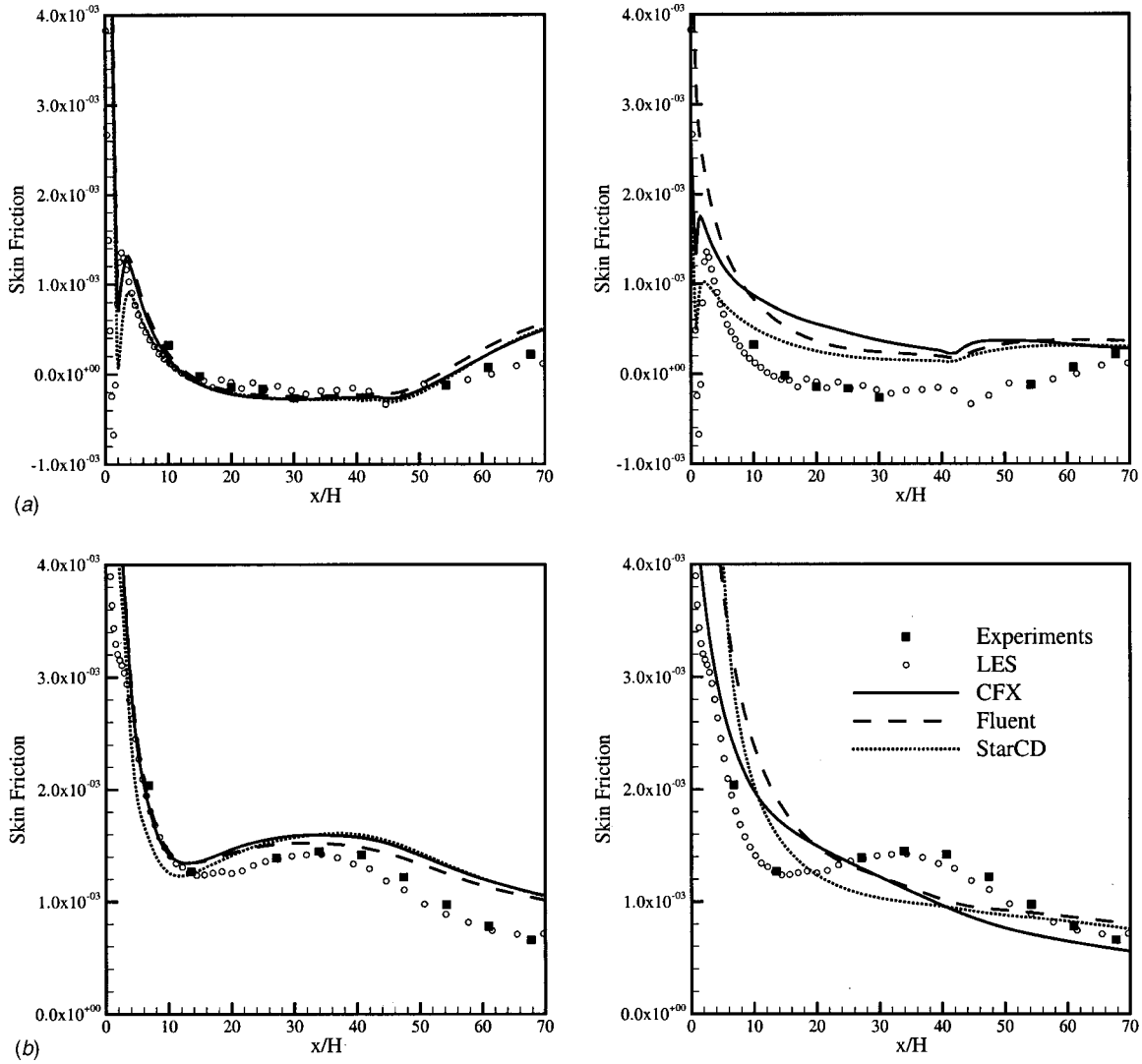

Fig. 7 Skin friction distribution on the diffuser walls. Left column: $\overline{v'^2}-f$ model; right column: low-Reynolds k-ϵ model. (a) Lower wall; (b) Upper wall.

any separation (as already noted). In addition, the three codes predicts quite different friction levels when the k-ϵ closure is employed.

In order to assess the grid sensitivity of the results presented, additional calculations on a refined grid were carried out. The grid was obtained by doubling the number of points in the two directions. The comparison between coarse and fine grid is reported in Fig. 8, in terms of mean flow velocity and turbulent kinetic energy profiles using Fluent and the low-Reynolds k-ϵ model. The results show that a grid converged solution has been reached. Similar comparisons are obtained for the other two codes. In addition, the results obtained using a high-order upwind discretization for the turbulent quantities are also reported on the same plots. The difference, in this case, is very small being the flow dominated by turbulence generation. This conclusion does not apply to more complex situations where the use of high-order differencing for the turbulent equations is mandatory.

The grid convergence study shows that the results obtained are not dependent on the grid and therefore, the differences in the streamwise velocity profiles in Fig. 5 and in the turbulent kinetic energy in Fig. 6, are not directly related to discretization accuracy or to the presence of artificial dissipation. One possible cause of the discrepancy between the codes is the presence of limiters/smoothers in the solution procedure. These operators are usually employed to *enforce* the positivity of selected quantities (turbulent variables, for example) and to improve convergence quality.

Additional simulations are performed using different turbulence models to explore capabilities of the CFD codes tested and the results are presented in Fig. 9. The standard k-ϵ model with the two-layer near-wall treatment gives results which are closely comparable to the predictions presented in Figs. 5 and 6 (using the damping functions). The separation on the bottom wall is not captured and the asymmetry in the turbulent kinetic energy profiles is very small. The two-layer treatment of the near-wall regions is available in both Fluent and StarCD and the results are comparable. On the other hand, the Nonlinear version of the Launder and Sharma k-ϵ model (available only in StarCD) captures the separation and gives a reasonably good representation of the turbulent kinetic energy. The results are in agreement with the experiments and close to the predictions of the $\overline{v'^2}-f$ model. These results are also in agreement with the data reported in the work by Apsley and Leschziner [5].

Finally, results are also presented for calculations with the DRSM model in low-Reynolds number form. This model is available in Fluent (in CFX only a High-Reynolds number version is available). The DRSM predictions do not show the expected improvement with respect to the standard k-ϵ model. This could be partly related to the near-wall treatment based on the two-layer

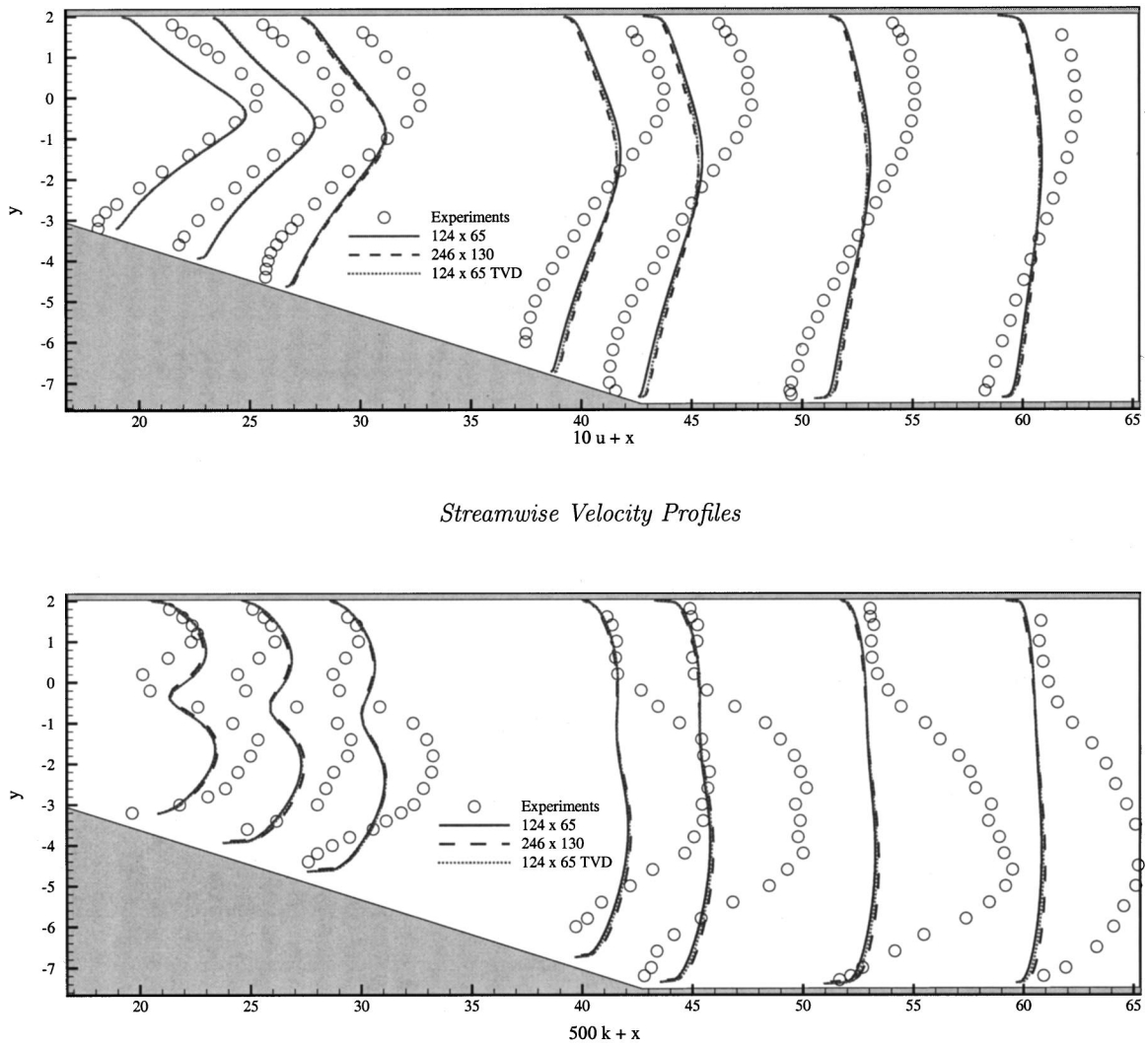

Fig. 8 Grid convergence and differencing scheme dependency—Fluent low-reynolds k-ϵ model

approach. Calculations performed in a similar configuration with the high-Reynolds version of the DRSM in Fluent [11] demonstrated good agreement with the experimental measurements.

It is worth noting that the two-layer k-ϵ required about the same amount of CPU as the Launder and Sharma model presented before and the convergence behavior was very similar. On the other hand, a slight increase in computational time is associated with the NLEV model and 25 percent more iterations were required to achieve the same drop in the residuals. The DRSM simulation required a CPU comparable with the $\overline{v'^2}-f$ one (the number of differential equations to be solved is the same for two-dimensional problems) but almost twice as many iterations were required to achieve convergence.

5 Conclusions

A comparison between three CFD commercial codes, namely CFX, Fluent, and Star-CD, is reported for turbulent flow in a planar asymmetric diffuser. Two turbulence models have been used. The first is the low-Reynolds number k-ϵ model (with Launder and Sharma damping functions) which is available as a standard feature in the codes. The second model is the $\overline{v'^2}-f$ model that has been implemented through the User Defined Routines in the three codes.

The same grid and the same spatial discretization have been used for all the simulations. In addition, a similar iterative procedure based on the SIMPLE technique has been used. In terms of convergence behavior, all the codes reach the steady-state approximately in the same number of iterations, regardless of the turbulence model used. The accuracy of the calculations as compared to the experimental and LES data is very good using the $\overline{v'^2}-f$ model. The length of the recirculation region is captured to within 6 percent and the skin friction on both walls agree reasonably well with the data. The negative velocity in the separation bubble is slightly underestimated. The results using the k-ϵ model do not show any recirculation. The flow is fully attached and this leads to a severe underprediction of the maximum velocity in the diffuser.

An effort was made to control all aspects of the simulations so that the same results were expected using different codes. In particular, the implementation of the $\overline{v'^2}-f$ turbulence model was carried out the same way in the three codes; indeed $\overline{v'^2}-f$ results do show an almost perfect agreement between CFX and Star-CD with Fluent being slightly more dissipative. The results using the k-ϵ model, on the other hand, show strong sensitivity to the code used. The model formulation is exactly the one proposed by Launder and Sharma, but the results are different (especially in terms of turbulent quantities and friction coefficients). This may be due to differences in implementation details which are not specified in the user manuals. In general, the differences between the k-ϵ results are much larger than those obtained using $\overline{v'^2}-f$, suggest-

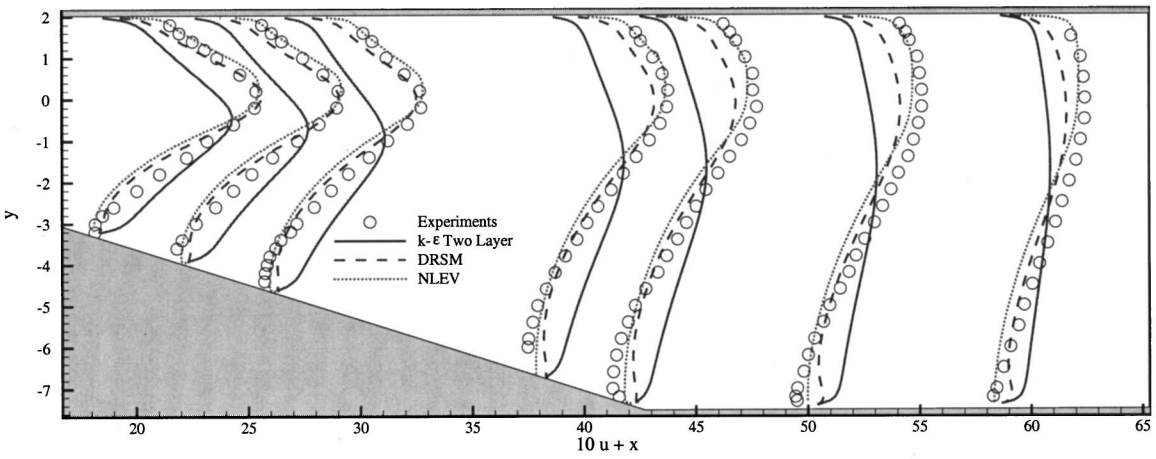

Streamwise Velocity Profiles

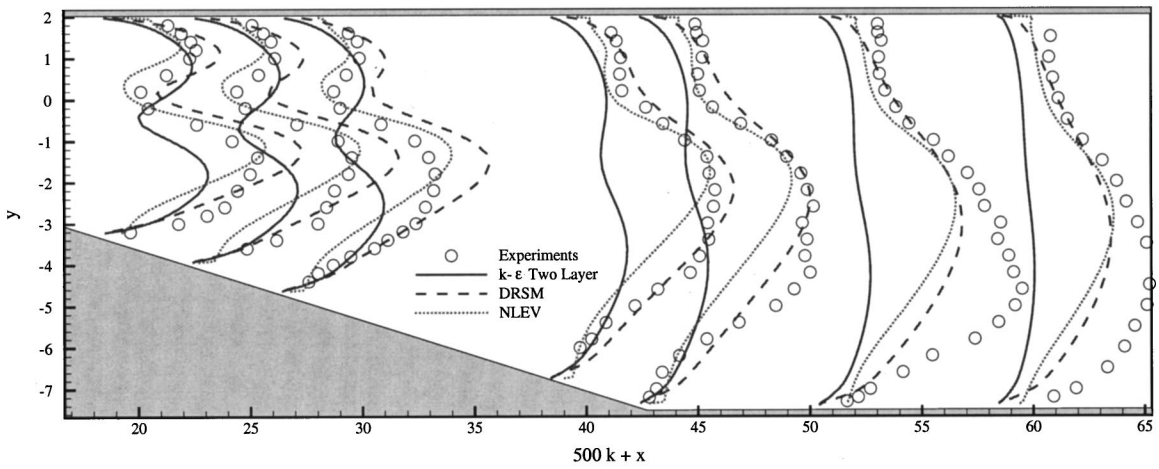

Turbulent Kinetic Energy Profiles

Fig. 9 Results using a differential Reynolds-stress model and non-linear eddy viscosity model

ing that the differences are less due to details of the numerical procedures in the codes than to the implementation of the turbulence models.

Today, one of the challenges in using commercial CFD codes is to choose between several physical/numerical models available. The cross comparison presented in this work proved that the basic numerical techniques (default options) are reliable and deliver the expected performance in terms of accuracy and convergence at least when the computational grid and the boundary conditions are defined carefully. On the other hand, the selection of the correct physical model (in this case the turbulence model) is crucial for the success of the simulations. Using one of the available turbulence models the results were not accurate and, in addition, not reproducible using different codes.

The $\overline{v'^2}-f$ model was implemented in CFX, Fluent, and StarCD *only* using the User Defined Routine feature. Even if the model is rather complex (involving three differential transport equations and a Helmotz-like equation) no particular difficulty was faced by the author. The performance of the codes was not compromised when compared with built-in models, and the expected accuracy level was reached with all the commercial codes tested. This demonstrates that the implementation of a customized physical model in an industrial tool is an available option for CFD practitioners thus shortening the distance between published research work and real–world applications.

Acknowledgments

The author wishes to thank A. Ooi for providing the initial implementation of the $\overline{v'^2}-f$ model in Fluent, and M. Fatica for providing the LES data for the diffuser; in addition, support for the implementation of the $\overline{v'^2}-f$ model was provided by P. Malan (Fluent Inc.), S. Jonnavithula (Adapco Ltd.), and H. Pordal (AEA Technologies Inc.). Discussion with P. Moin, P. Durbin, and G. Medic are appreciated.

References

[1] Freitas, C. J., 1995, "Perspective: Selected Benchmarks From Commercial CFD Codes," ASME J. Fluids Eng., **117**, p. 210–218.
[2] Durbin, P. A., 1996, "On the k-ϵ Stagnation Point Anomaly," Int. J. Heat Fluid Flow, **17**, pp. 89–91.
[3] Launder, B. E., and Sharma, A., 1974, "Application of the Energy-Dissipation Model of Turbulence to the Calculation of Flow Near a Spinning Disk," Lett. Heat Mass Transfer **1**, pp. 131–138.

[4] Durbin, P. A., 1995, ''Separated Flow Computations with the k-ϵ-v^2 Model,'' AIAA J., **33**, pp. 659–664.
[5] Apsley, D. D., and Leschziner, M. A., 2000, ''Advanced Turbulence Modeling of Separated Flow in a Diffuser,'' Flow, Turbul. Combust., **63**, pp. 81–112.
[6] Parneix, S., Durbin, P. A., and Behnia, M., 1998, ''Computation of a 3D turbulent boundary layer using the $\overline{v'^2}-f$ model,'' Flow, Turbul. Combust., **10**, pp. 19–46.
[7] Behnia, M., Parneix, S., Shabany, Y., and Durbin, P. A., 1999, ''Numerical Study of Turbulent Heat Transfer in Confined and Unconfined Impinging Jets,'' Int. J. Heat Fluid Flow **20**, pp. 1–9.
[8] Kaltenback, H. J., Fatica, M., Mittal, R., Lund, T. S., and Moin, P., 1999, ''Study of the Flow in a Planar Asymmetric Diffuser Using Large Eddy Simulations,'' J. Fluid Mech., **390**, pp. 151–185.
[9] Vandoormaal, J. P., and Raithby, G. D., 1984, ''Enhancements of the SIMPLE Method for Predicting Incompressible Fluid Flows,'' Numer. Heat Transfer, **7**, pp. 147–163.
[10] Leonard, B. P., 1979, ''A Stable and Accurate Convective Modeling Procedure Based on Quadratic Upstream Interpolation,'' Comput. Methods Appl. Mech. Eng., **19**, pp. 59–98.
[11] Kim, S. E., 2001, ''Unstructured Mesh Based Reynolds Stress Transport Modeling of Complex Turbulent Shear Flows,'' AIAA Paper 2001-0728.
[12] Barth, T. J., and Jespersen, D., 1989, ''The Design and Application of Upwind Schemes on Unstructured Meshes,'' AIAA Paper 89-0366.
[13] Craft, T. J., Launder, B. E., and Suga, K., 1995, ''A Non-Linear Eddy-Viscosity Model Including Sensitivity to Stress Anisotropy,'' *Proc. 10th Symposium on Turbulent Shear Flows*, **2**, pp. 23.19–23.24.
[14] Launder, B. E., and Spalding, D. B., 1972, *Mathematical Models of Turbulence*, Academic Press, London.
[15] Rodi, W., 1991, ''Experience with two-layer models combining the k-ϵ model with a one-equation model near the wall,'' AIAA Paper 91-0216.
[16] Gibson, M. M., and Launder, B. E., 1978 ''Ground Effects and Pressure Fluctuations in the Atmospheric Boundary Layer,'' J. Fluid Mech., **86**, pp. 491–511.
[17] Speziale, C. G., Abid, R., and Anderson, E. C., 1990, ''A critical evaluation of two-equation models for near wall turbulence,'' AIAA Paper 90-1481.
[18] Obi, S., Aoki, K., and Masuda, S., 1993, ''Experimental and Computational Study of Turbulent Separating Flow in an Asymmetric Plane Diffuser,'' *Proc. 9th Symposium on Turbulent Shear Flows*, pp. 305-312.
[19] Buice, C. U., and Eaton, J. K., 1997, ''Experimental Investigation of Flow Through an Asymmetric Plane Diffuser,'' Report No. TSD-107. Thermosciences Division, Department of Mechanical Engineering, Stanford University, Stanford, CA, USA.